CHEMMEDCHEM

DOI: 10.1002/cmdc.200700082

AT_1 Receptor Ligands: Virtual-Screening-Based Design with TOPP Descriptors, Synthesis, and Biological Evaluation of Pyrrolidine Derivatives

Claudia Lamanna,[a, b] Alessia Catalano,[a] Alessia Carocci,[a] Antonia Di Mola,[a] Carlo Franchini,*[a] Vincenzo Tortorella,[a] Patrick M. L. Vanderheyden,[c] Maria S. Sinicropi,[d] Kimberly A. Watson,[b] and Simone Sciabola[e]

*As a continuing effort to establish the structure–activity relationships (SARs) within the series of the angiotensin II antagonists (sartans), a pharmacophoric model was built by using novel TOPP 3D descriptors. Statistical values were satisfactory (PC4: $r^2 = 0.96$, $q^2_{(5\ random\ groups)} = 0.84$; SDEP = 0.26) and encouraged the synthesis and consequent biological evaluation of a series of new pyrrolidine derivatives. SAR together with a combined 3D quantitative SAR and high-throughput virtual screening showed that the newly synthesized 1-acyl-*N*-(biphenyl-4-ylmethyl)pyrrolidine-2-carboxamides may represent an interesting starting point for the design of new antihypertensive agents. In particular, biological tests performed on CHO-hAT_1 cells stably expressing the human AT_1 receptor showed that the length of the acyl chain is crucial for the receptor interaction and that the valeric chain is the optimal one.*

Introduction

Despite the availability of a large number of agents for treating hypertension, approximately one-third of the hypertensive population is still not adequately treated.[1] The renin–angiotensin system (RAS) plays a key role in the pathophysiology of hypertension,[2] and the octapeptide hormone angiotensin II (Ang II) is the primary vasoconstrictor agent produced by this system. Inhibition of the RAS by renin inhibitors, angiotensin-converting enzyme (ACE) inhibitors, and Ang II receptor antagonists continues to be the most active area of drug discovery for the treatment of hypertension, congestive heart failure, and possibly chronic renal failure.[3] ACE inhibitors such as enalapril and captopril are largely used in the clinic for the treatment of hypertension. However, ACE is not a selective enzyme, as it possesses among its substrates important peptides such as bradykinin and substance P; thus, the clinical use of ACE inhibitors is accompanied by several side effects, such as dry cough, angioedema, and rushes.[4] Therefore the specific block of Ang II activity at the receptor level represents a potentially convenient approach to modulate the RAS and to avoid side effects. Two Ang II receptor subtypes, called AT_1 and AT_2, were cloned and characterized.[5,6] The AT_1 receptor is a G-protein-coupled receptor[6,7] and mediates the majority of the known physiological effects of Ang II, most of which are those associated with the cardiovascular system and the kidney;[3] much less is known about the function and intracellular functional response coupled to the AT_2 receptor.[8] The discovery of the first potent and orally active nonpeptide AT_1-selective antagonist losartan[9] generated significant interest in the search for other nonpeptide Ang II antagonists bearing novel heterocyclic elements,[10] and many other sartans, derivatives of losartan (such as irbesartan or valsartan), appeared for the treatment of hypertension in the last 10 years (Figure 1). Most of these compounds have a biphenyl fragment bearing an acidic moiety in common and differ in the nature of the pendent heterocyclic system connected to the *para* position of the distal phenyl ring by means of a methylene group. In the absence of 3D structural data, numerous 3D QSAR and modeling studies on Ang II and its binding to the AT_1 receptor have been performed.[11–15] The most reliable hypothesis for the receptor interaction shows that the key elements are represented by: a bulky substituent, an alkyl chain, and a biaromatic structure

[a] *Dr. C. Lamanna,[+] Dr. A. Catalano, Dr. A. Carocci, Dr. A. Di Mola, Prof. C. Franchini, Prof. V. Tortorella*
Dipartimento Farmaco-Chimico, Università degli Studi di Bari
Via E. Orabona 4, 70125 Bari (Italy)
Fax: (+39) 080-5442724
E-mail: cfranc@farmchim.uniba.it

[b] *Dr. C. Lamanna,[+] Dr. K. A. Watson*
The BioCenter, Whiteknights P.O. Box 221
Reading, Berkshire, RG6 6AS (UK)

[c] *Prof. P. M. L. Vanderheyden*
Department of Molecular and Biochemical Pharmacology
Vrije Universiteit Brussel, 1050 Brussels (Belgium)

[d] *Prof. M. S. Sinicropi*
Dipartimento di Scienze Farmaceutiche, Università della Calabria
87036 Arcavacata di Rende (CS) (Italy)

[e] *Dr. S. Sciabola*
Laboratorio di Chemiometria, Università di Perugia
Via Elce di Sotto 10, 06123 Perugia (Italy)

[+] *Present address:*
Siena Biotech S.p.A., Drug Profiling Unit
Via Fiorentina 1, 53100 Siena (Italy)

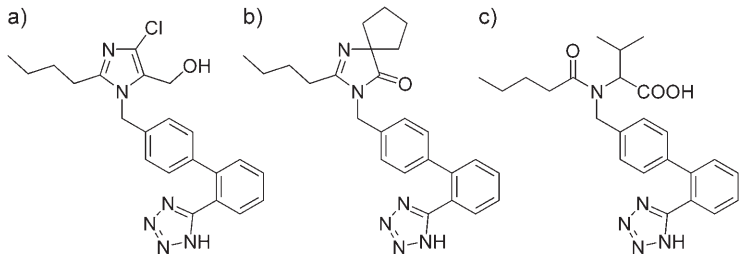

Figure 1. Structures of a) losartan, b) irbesartan, and c) valsartan.

able to fit into three lipophilic pockets of the AT_1 receptor; a moiety that can undergo a hydrogen bonding interaction with the AT_1 receptor; a heterocyclic nitrogen atom that acts as hydrogen bond acceptor; and an acidic group that is able to interact with the basic Lys 199 residue of the transmembrane helix 5 (TM5) of the AT_1 receptor (Figure 2).[10,16,17] The ionic interactions may be significant because of their long-range effects, and hydrophobic aromatic areas should be important for stabilization of the acid–base interaction by diminishing the dielectric effect of water.[18] Three common features were found in all 3D QSAR models: an electron-rich site and two π-electron-rich sites, corresponding to oxygen or chlorine atoms and the phenyl rings, respectively.[15] The *ortho* position of the acidic substituent seems to be important for twisting the biphenyl groups out of coplanarity.[14] The design of new nonpeptide Ang II antagonists followed a pharmacophoric model built with a novel 3D pharmacophore fingerprinting approach, TOPP (triplets of pharmacophoric points), which proved to be a powerful high-performance method for virtual screening.[19] This modeling study confirmed the finding that the opening of the imidazole ring did not lead to the loss of AT_1 receptor affinity, as it had previously been described for valsartan.[20] Moreover, the superimposition of losartan and irbesartan (Figure 3) shows that it is not the hydrogen atom of the hydroxy group (such as in losartan) that is relevant for the interaction, but the lone pair of the oxygen itself (the carbonyl and the hydroxy groups occupy the same region in space, despite the methylene group of losartan).[21] Hence, by superimposing losartan onto one of the structures that came out of the virtual screening protocol implemented in our analysis (compound **Ic**, Figure 4), we found that the tertiary amido carbonyl function of this compound could have been potentially placed in the same pivotal position occupied by the hydroxy oxygen atom of losartan (Figure 5a). Moreover, based on isosteric relationship considerations, the pyrrolidine cycle of **Ic** could be potentially used to replace the cyclopentyl moiety of irbesartan (Figure 5b). These findings formed the basis for the synthesis of new analogues related to

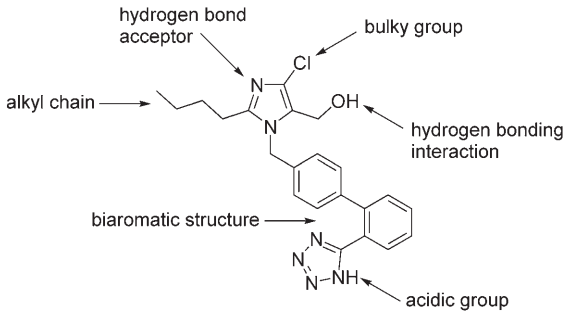

Figure 2. Pharmacophore features for the sartan compound class based on the structure of DuP-753 (losartan).[10]

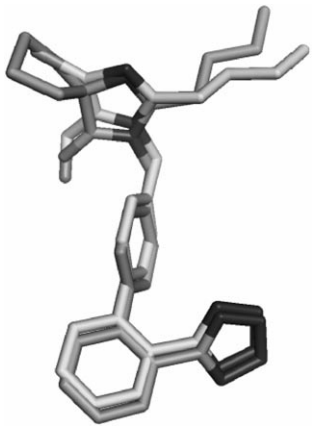

Figure 3. Superimposition of losartan (light gray) with irbesartan (darker gray).

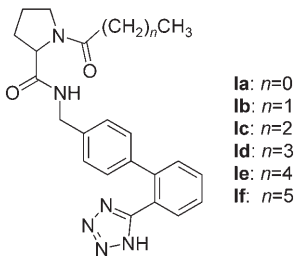

Figure 4. Newly synthesized 1-acyl-*N*-(biphenyl-4-ylmethyl)pyrrolidine-2-carboxamides.

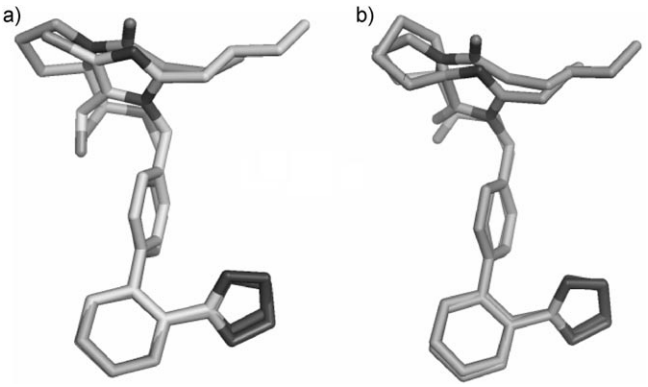

Figure 5. Superimposition of a) losartan (light gray) and **Ic**, and b) irbesartan and **Ic**.

this compound (**Ia–f**, Figure 4). In this way, the bulky substituent of sartans (the chlorine atom of losartan and the spirocyclic group of irbesartan) is mimicked by the pyrrolidine group, the nitrogen atom at the 3-position of the imidazole ring of losartan and irbesartan is replaced by a carbonyl group (as for valsartan),[10] and the alkyl chain of losartan, irbesartan, and valsartan is replaced by an acyl chain.

Methods

Dataset

The dataset selected for this work (Table 1) consisted of 49 AT_1 antagonists, previously described by Yoo et al.[22] and by Le Bourdonnec et al.[23] The 3D structures of the training set were generated in their non-ionized form and minimized with the software SYBYL[24] using the MMFF force field parameterized in vacuo. Structural modifications mainly refer to substitution in the imidazole ring while keeping the tetrazole–biphenyl scaffold, representative of the most common therapeutic compounds. The activity data were taken from the available literature, where equivalent binding assays using the human AT_1 receptor are described.[22,23] The activities are reported as K_i values, which range from 0.31 to 158.0 nM. For 3D QSAR studies, training ($n=41$) and test ($n=8$) sets were built. The "Most Descriptive Compound" option available in the software GOLPE[25] was used to automatically select a balanced and chemically diverse test set based on TOPP descriptors. Training and test set structures are listed in Table 1, where members of the test set are represented by underlined values.

Table 1. Dataset structures.[a]

Entry	K_i [nM]	Structure	Entry	K_i [nM]	Structure
irbesartan	2.5	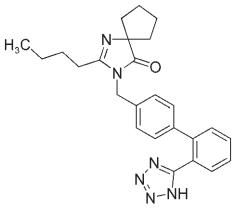	25	10.71	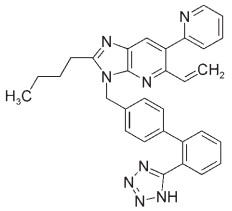
01	0.69	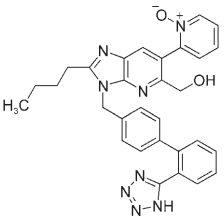	<u>26</u>	<u>4.25</u>	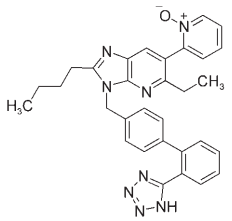
<u>02</u>	<u>0.69</u>	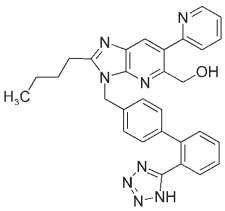	27	1.81	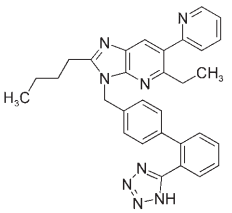
03	1.18	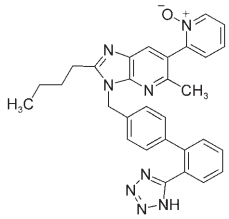	28	1.19	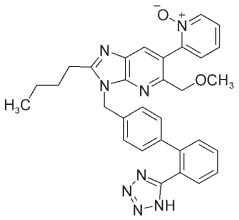
04	1.31	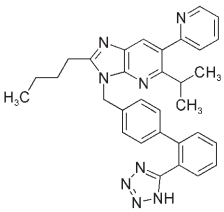	29	6.63	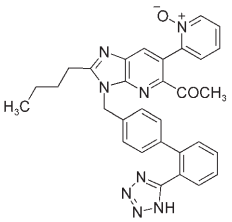
05	1.50	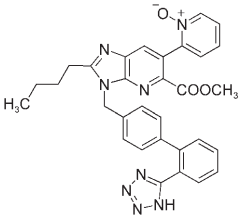	30	1.50	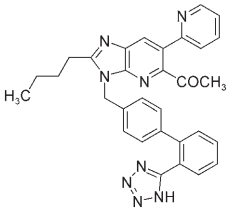
06	1.57	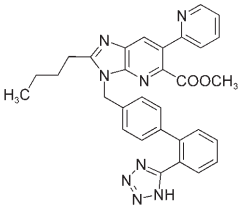	31	3.76	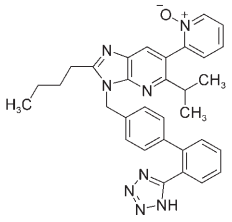

Table 1. (Continued)

Entry	K_i [nM]	Structure	Entry	K_i [nM]	Structure
07	1.23	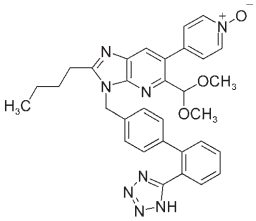	32	10.7	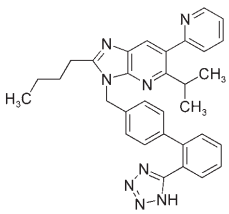
08	1.14	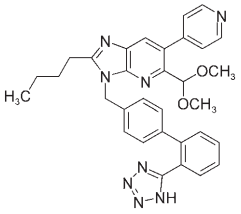	33	10.1	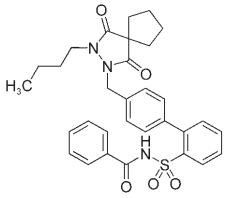
09	0.72	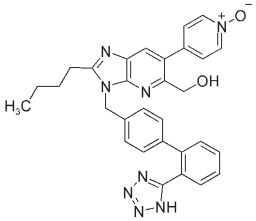	34	43.7	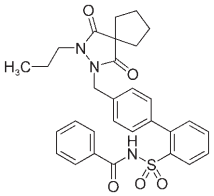
10	0.89	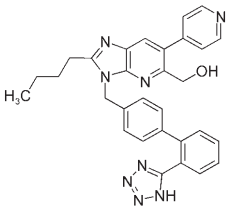	35	23.5	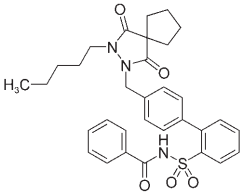
11	0.77	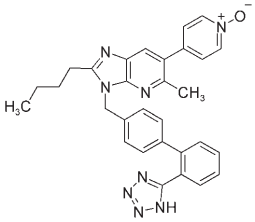	36	21.8	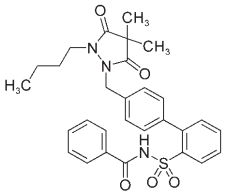
12	2.08	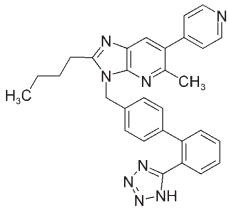	37	27.7	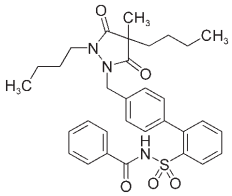
13	0.87	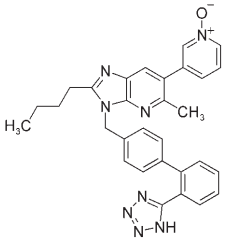	38	18.5	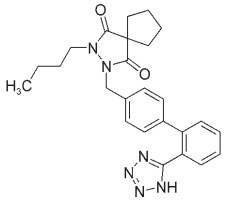

Triplets of pharmacophoric points (TOPP) descriptors

TOPP is a QSAR approach that uses 3-point pharmacophores as 3D descriptors and GOLPE to perform multivariate statistical analysis.[19] The working protocol carried out by TOPP is represented in Figure 6. First, the atoms of each molecule are classified by the GRID force field parameterization. In this way, atoms are described according to their charge and hydrogen bonding properties: DRY (hydrophobic), DONN (HBD, hydrogen bond donor), ACPT (HBA, hydrogen bond acceptor) and DNAC (both HBD and HBA). After classification of the atoms, an iterative procedure generates all the possible combinations of three points and four different atom types (DRY, DONN, ACPT, and DNAC), encoding them in two possible ways: one approach is to store only the presence or absence of a 3-point pharmacophore combination, whereas the other consists of counting the number of times a combination is present in the molecule. The calculations described above are performed for all the compounds, and the results, that is, the combinations of 3-point pharmacophores, are stored in an *X*-matrix of descriptors. As this final matrix of descriptors is built up in a dynamic way, no length of the bit string is initially fixed. When the first compound is processed, the first row of the *X*-matrix consists exclusively of those variables present in this compound. Therefore, all the bits so far are set to "1". When the program processes the second compound, the *X*-matrix will change according to the triangles present in this second compound. Then, the program will fill with "0"s these new positions in the first row (compound 1) due to the processing of the second compound and also the

Table 1. (Continued)

Entry	K_i [nM]	Structure	Entry	K_i [nM]	Structure
14	2.17	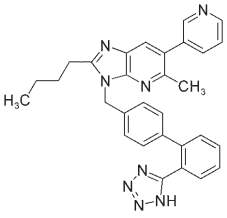	39	11.8	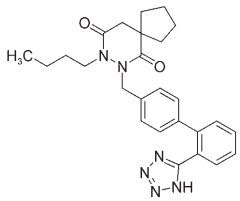
15	1.23	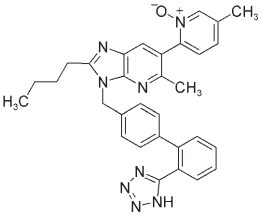	40	23.8	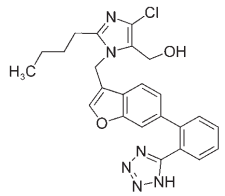
16	1.79	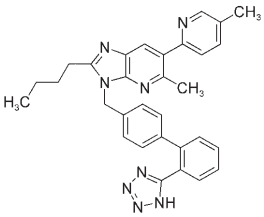	41	27.2	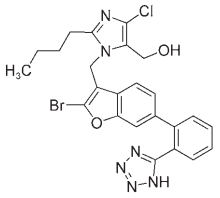
17	1.35	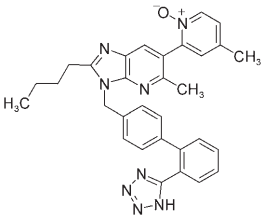	42	14.9	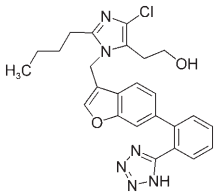
18	0.31	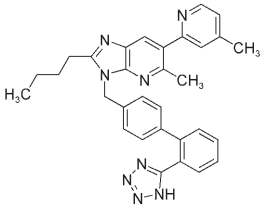	43	42.5	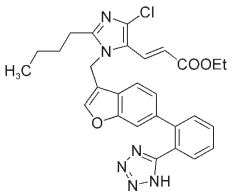
19	1.11	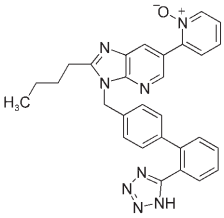	44	23.3	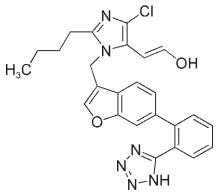
20	1.14	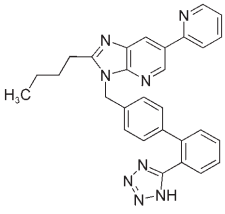	45	27.5	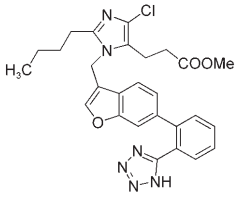

positions of the second row due to the first compound.[19] The final *X*-matrix is submitted for statistical analysis, that is, a linear regression model using principal components analysis (PCA) and partial least squares (PLS).

Descriptors derived for database clustering

Database mining strictly depends on the selection of appropriate molecular descriptors, guided by the specific aim of a study. Pharmacokinetic and pharmacodynamic aspects of database mining are treated, including the VolSurf[26] descriptors and the GRid INdependent Descriptors (GRIND).[27] Both types of descriptors start from molecular interaction fields (MIF) computed with the program GRID. The large body of information contained in these fields (on the order of $\sim 10^5$ grid points) is then encoded using two different methods. VolSurf analyzes the MIF obtained with diverse probes (often water and the hydrophobic probe) and computes the volume and surface of the regions that encompass interaction energy values under certain cutoff limits, together with some other variables that express their geometric distributions in space. The result of such an analysis is a small number of variables describing the overall distribution of hydrophobic and hydrophilic regions around the molecule, with a distinct physicochemical meaning. VolSurf descriptors are useful for describing pharmacokinetic and physicochemical properties.[26] On the other hand, GRIND descriptors have been designed mainly to represent pharmacodynamic properties. The computation of GRIND involves a preliminary simplification of a few MIF to extract the main pharmacophoric regions,

Table 1. (Continued)

Entry	K_i [nM]	Structure	Entry	K_i [nM]	Structure
21	1.76	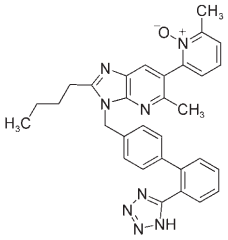	46	52.9	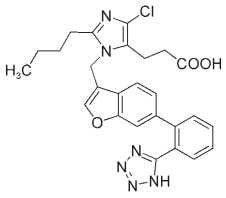
22	2.13	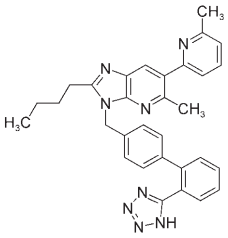	47	13.0	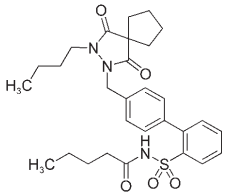
23	1.60	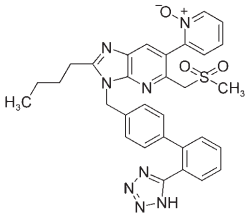	48	32.0	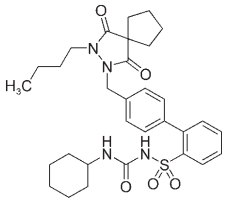
24	0.76	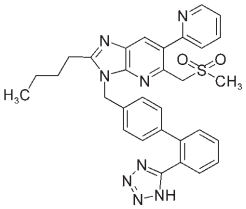	49	158.0	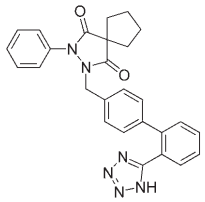

[a] Underlined entries represent members of the test set. They were selected according to the "Most Descriptive Compound" option available in the software GOLPE.

followed by a particular type of autocorrelating transformation. The results are a small set of alignment-independent descriptors that represent the internal geometrical relationship of such pharmacophoric regions. These can be used directly for chemometric analysis and can be interpreted with the appropriate software by using graphical representations of the pharmacophoric regions and their interactions, together with the molecular structures, in interactive 3D plots.

Statistical analysis

PCA and PLS analyses were performed with the software GOLPE. Scaling was applied according to the descriptor type. The optimal dimensionality of the PLS model was chosen according to the cross-validation results. In our analysis, all computations were performed on a Pentium IV PC with 3 gigabytes of main memory.

Selecting compounds on pharmacophore-derived descriptors

Compound conformations were obtained by modeling the structures within SYBYL. Compound 01 (Table 1) was used as a template for alignment of the whole dataset, carried out by superimposing the common (tetrazole–biphenyl) scaffold and then optimizing the remaining parts of the molecules (Figure 7). All the structures were further minimized using the SYBYL force field by applying the Powell method, with 1000 as the maximum number of iterations together and keeping all the other parameters as standard. After every compound was superimposed, TOPP descriptors were derived for all training set compounds; in turn, fractional factorial design (FFD) was used to select the variables for the *X*-space, which finally amounted to 321 TOPP descriptors, as well as to define the dimensionality of the PLS model, being optimal with four latent variables. This explained 96% of the variance with a standard deviation of the error of calculation (SDEC) = 0.14. For internal validation, five random groups were used and $q^2 = 0.84$ and a standard deviation of the error of prediction (SDEP) = 0.26 were obtained. For external validation, eight test set compounds were projected and a SDEP of 0.15 was achieved. The prediction of the test set is represented graphically in Figure 8. All the compounds were satisfactorily predicted, showing how TOPP fingerprints can be used to efficiently rank molecules for QSAR purposes. The model was then used for virtual screening analysis performed on a subset of a large database made of ~55000 compounds collected together by merging ~53000 compounds from Maybridge[28] plus ~2000 in-house compounds from the collections at the University of Perugia and the University of Bari. To perform the virtual screening analysis only on a subset of the original database, compounds were clustered based on ALMOND and VolSurf 3D descriptors. To help us focus on a region in PC space based on the pharmacophoric (ALMOND) and physicochemical (VolSurf) properties where new potential sartan derivatives could be found, the original database was enriched by including the studied dataset of sartans (gray square symbols in Figure 9). Indeed, a restricted area was recognized, and within this area 250 compounds were extracted

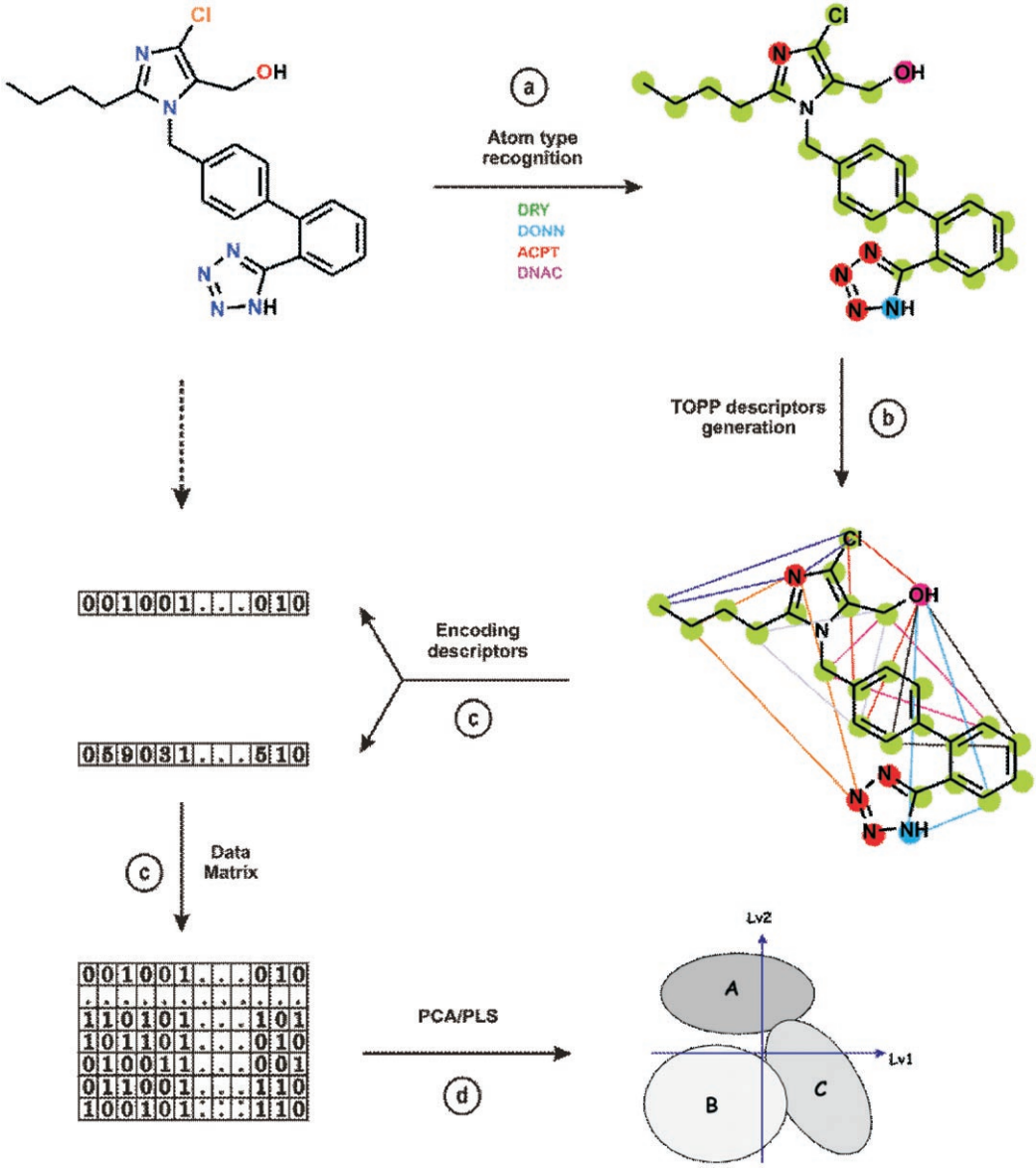

Figure 6. a) the atoms of each molecule are classified by the GRID force field parameterization. In this way, atoms are described according to their charge and hydrogen bonding properties: DRY (hydrophobic), DONN (HBD, hydrogen bond donor), ACPT (HBA, hydrogen bond acceptor) and DNAC (both HBD and HBA). b) after atom classification an iterative procedure generates all possible combinations of triplets with the four different atom types (DRY, DONN, ACPT, and DNAC). c) these triplets of pharmacophoric points (TOPP) are calculated for all database compounds and stored in an *X*-matrix of descriptors. d) the final *X*-matrix is submitted for statistical analysis: a linear regression model using principal components analysis (PCA) and partial least squares (PLS) analysis.

with the criterion "Most Descriptive Compound" (MDC) as implemented in GOLPE.[25] For every selected molecule, a maximum of 100 conformations were generated using an in-house conformational analysis scheme and then projected on the TOPP–PLS model. Among the computed conformers, each database molecule was given a score reflecting the highest predicted value of pK_i obtained by one of its conformers, and this score was finally used to rank the whole set of the 250 extracted molecules.

Cell culture and [^{3}H]valsartan binding

Chinese hamster ovary cells (CHO-K1) stably transfected with the human angiotensin II AT_1 receptor (denoted as CHO-AT_1 cells)[29] were cultured in 24-well plates in Dulbecco's modified essential medium (DMEM) supplemented with L-glutamine (2 mM), 2% of a stock solution containing penicillin (5000 IU mL^{-1}) and streptomycin (5000 μg mL^{-1}) (Life Technologies, Merelbeke, Belgium), and 10% fetal bovine serum (Life Technologies, Merelbeke, Belgium). The cells were grown in 5% CO_2 at 37 °C until confluent, and before binding experiments, were washed three times with 0.5 mL well^{-1} of DMEM at room temperature. The cells were then incubated at 37 °C

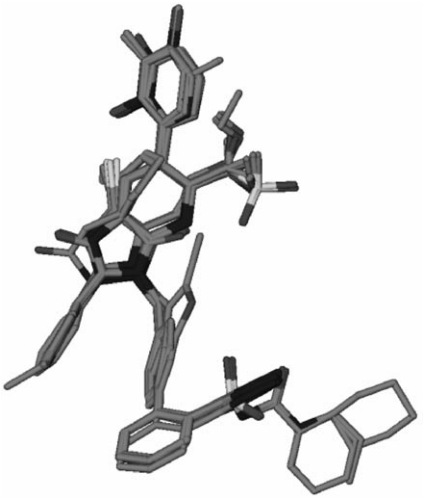

Figure 7. Alignment of all the training set ligands taking compound 01 as a template and then superimposing the common tetrazole–biphenyl scaffold.

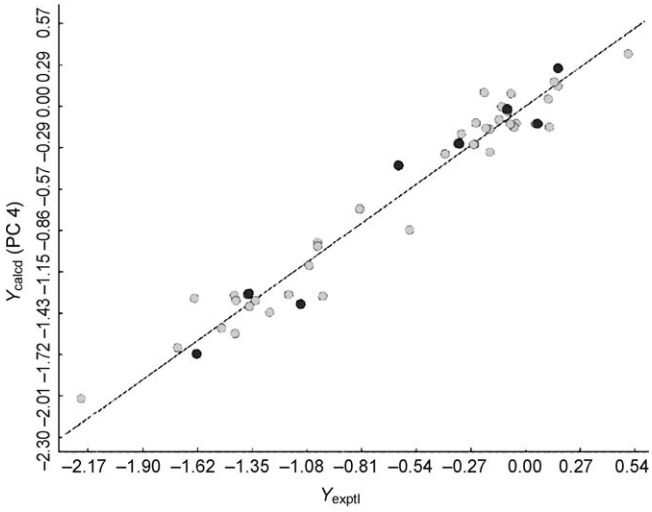

Figure 8. The use of TOPP descriptors in PLS analysis of the training set compounds ($n = 41$) resulted in a QSAR model, being optimal with four latent variables (gray circles). These explained 96% of the variance with SDEC = 0.14. Internal validation gave $q^2 = 0.84$ and SDEP = 0.26. For external validation of eight test compounds (black circles) a SDEP of 0.15 was achieved.

for 30 min in a final volume of 0.5 mL in each well containing 400 μL DMEM, 50 μL DMEM containing the investigated compound at increasing final concentrations between 10^{-9} and 10^{-5} M, and 50 μL [^{3}H]valsartan at a final concentration of 1.5 nM. At the end of the incubation, the cells were placed on ice and washed three times with ice-cold PBS containing $CaCl_2 \cdot 2H_2O$ (0.132 g L^{-1}), KCl (0.2 g L^{-1}), KH_2PO_4 (0.2 g L^{-1}), $MgCl_2 \cdot 6H_2O$ (0.1 g L^{-1}), NaCl (8 g L^{-1}), and $Na_2HPO_4 \cdot 2H_2O$ (1.44 g L^{-1}). To measure radioligand binding, 0.5 mL 1 M NaOH was added to the cells and then transferred into scintillation vials containing 3.5 mL scintillation liquid (Optiphase "Hisafe2", PerkinElmer). The binding values were normalized with total binding (that is, in the absence of competing ligand) and non-

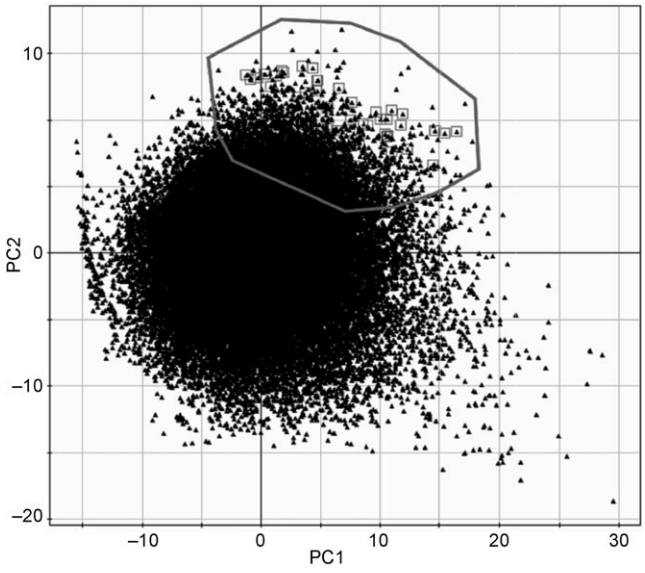

Figure 9. PCA scores plot highlighting the subset region selection performed with the "Most Descriptive Compound" clustering procedure available in GOLPE.

specific binding (in the presence of the potent AT_1 receptor antagonist candesartan at 1 μM). IC_{50} values were determined by nonlinear regression analysis of the competition curves using GraphPad Prism and were converted into the corresponding K_i values as previously described.[30]

Results and Discussion

From the molecular modeling studies described above, one of our internal structures, namely **Ic**, was found among the compounds with a higher score (Figure 10). This compound presented the required structural features for binding to the AT_1 receptor. In fact, superimposition of **Ic** with irbesartan shows

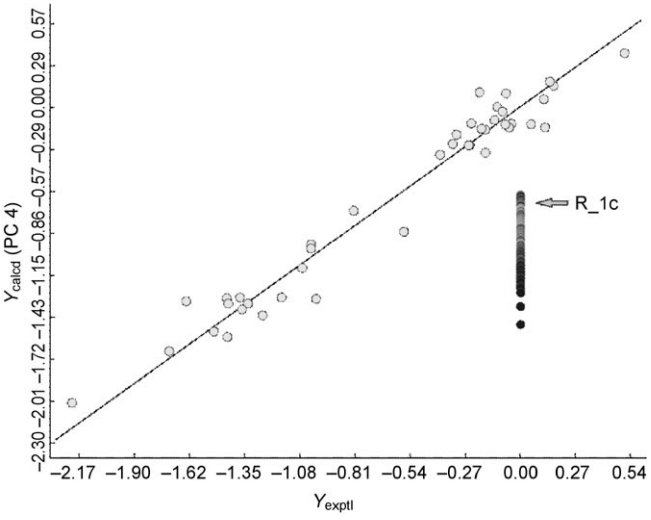

Figure 10. The final step in our virtual screening protocol. The PLS predictions plot shows the calculated activity values for the compounds selected by clustering the Maybridge/in-house database.

that the two carbonyl oxygen atoms occupy the same area as previously described for the hydroxy group of losartan and that the pyrrolidine ring overlaps with the cyclopentyl moiety of irbesartan; it is also bulky enough to substitute the chlorine atom of losartan (Figure 5). Moreover, the tertiary amido carbonyl function of **Ic** occupies the same area of the nitrogen atom at the 3-position of the imidazole (or imidazoline) ring of the sartans considered. In addition, the acyl chain of **Ic** offers a hydrogen bond interaction (carbonyl moiety), making an insightful understanding of other potential electrostatic interactions possible. For the reasons discussed above, we decided to focus on this particular scaffold and when tested, compound **Ic** showed an IC_{50} value of 10 μM ($K_i = 3.9$ μM) (Table 2). Starting from this molecule, we designed an initial small set of compounds in which the length of the alkyl side chain was varied (Figure 4). Compounds **Ia**–**f** were prepared by the synthetic routes shown in Scheme 1. Bromination of the commercially available nitrile **1** with *N*-bromosuccinimide[9] provided compound **2**, which was submitted to a Gabriel reaction to give the phthalimido derivative **3**. Deprotection of the amino function by cleavage of the phthalimido group with hydrazine[31] gave compound **4**, which was submitted to condensation with (±)-1-(*tert*-butoxycarbonyl) pyrrolidine-2-carboxylic acid[32] in the presence of 2-ethoxycarbonyl-1,2-dihydroquinoline (EEDQ)[33,34] to afford compound **5** in good yield. Deprotection of compound **5** with 48% HBr gave compound **6**, which was converted into the acyl derivatives **7a**–**f**, either by reaction with acetyl chloride (for **7a**), or with propionic, butyric, valeric, hexanoic, and heptanoic acids, respectively (for **7b**–**f**) under different reaction conditions (see Experimental Section). Compounds **7a**–**f** were converted into their corresponding trimethyltin tetrazole derivatives **8a**–**f** by reaction with azidotrimethyltin. Compounds **Ib**–**f** were obtained by treatment of **8b**–**f** with gaseous HCl.[35] Compound **Ia** was directly obtained by column chromatography of **8a**, following a procedure reported in the literature.[36] Reaction of compound **5** with azidotrimethyltin gave its trimethyltin tetrazole derivative along with unreacted **5**. Purification of the mixture as such by column chromatography gave compound **9**. The compounds described herein were tested on CHO cells stably transfected with human AT_1 receptor cDNA (CHO-hAT_1). The receptor binding affinity was measured by the ability to displace [^{3}H]valsartan from its specific binding sites. The binding data of the tested compounds are shown in Table 2. The results are in agreement with the molecular modeling studies, as they showed that our hypothesis is correct. Hence, the secondary amido carbonyl group of the tested compounds might be positioned in a favorable orientation to mimic the hydroxymethyl group of losartan or the carbonyl group of irbesartan (see Figure 5 for **Ic**). Moreover, the tertiary amido carbonyl group of the tested compounds might mimic the nitrogen atom at the 3-position of the imidazole and imidazolinone moieties of losartan and irbesartan, respectively, and it undergoes a specific hydrogen

Table 2. AT_1 binding properties of newly synthesized compounds.

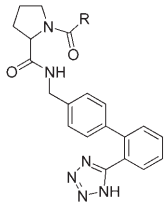

Compd	R	K_i [μM][a]
(*R*,*S*)-**Ia**	CH_3	>10
(*R*,*S*)-**Ib**	CH_2CH_3	>10
(*R*,*S*)-**Ic**	$(CH_2)_2CH_3$	3.9
(*R*,*S*)-**Id**	$(CH_2)_3CH_3$	0.60
(*R*,*S*)-**Ie**	$(CH_2)_4CH_3$	0.83
(*R*,*S*)-**If**	$(CH_2)_5CH_3$	1.76
(*R*,*S*)-**9**	$OC(CH_3)_3$	>10
losartan		0.0158[b]
irbesartan		0.00148[b]
valsartan		0.00128[b]

[a] Affinities were calculated from competition curves by using nonlinear regression analysis and GraphPad Prism. [b] See Ref. [30].

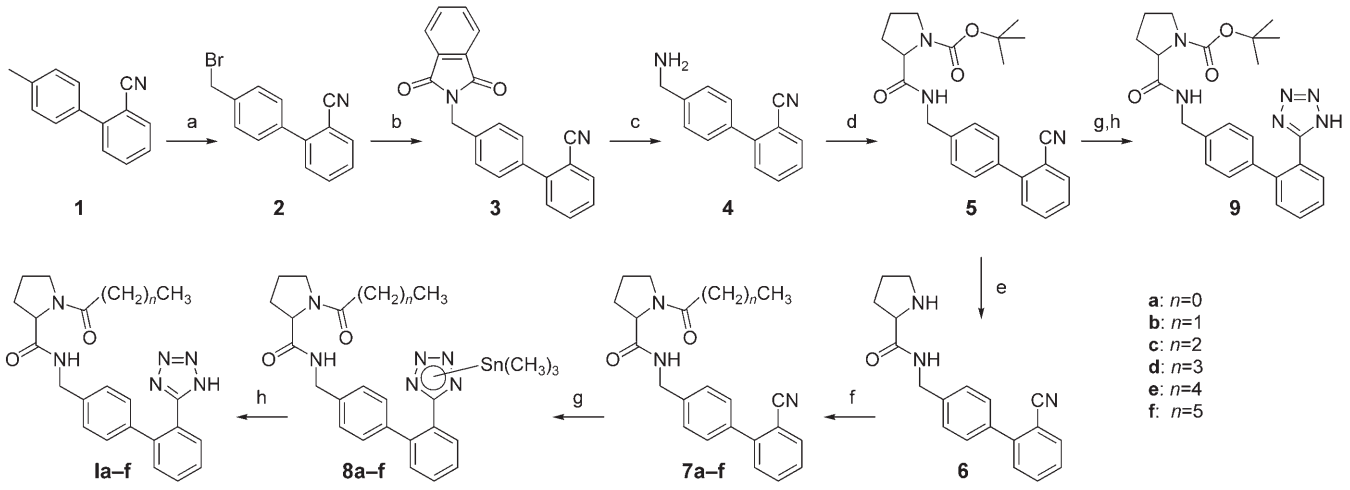

Scheme 1. Reagents and conditions: a) *N*-bromosuccinimide, $(PhCO)_2O_2$, CCl_4, reflux; b) potassium phthalimide, DMF, reflux; c) $N_2H_4{\cdot}H_2O$ (98%), MeOH/EtOH (abs), reflux; d) (*R*,*S*)-1-(*tert*-butoxycarbonyl)pyrrolidine-2-carboxylic acid, EEDQ, Et_3N, $CHCl_3$, reflux; e) HBr (48%), EtOAc, room temperature; f) CH_3COCl, Et_3N, toluene, reflux (for **7a**); $CH_3(CH_2)_nCOOH$ (for **7b**–**d**), EEDQ, Et_3N, $CHCl_3$, reflux; $CH_3(CH_2)_nCOOH$, $SOCl_2$, Et_3N, THF (for **7e**,**f**); g) $(CH_3)_3SnN_3$, toluene, reflux; h) silica gel (for **9** and **Ia**); HCl (g), toluene/THF (for **Ib**–**f**).

bond interaction with a donor residue of the AT_1 receptor. Furthermore, the variation in affinity among tested compounds shows that the length of the acyl side chain on the pyrrolidine scaffold is critically important for these compounds to establish a good fit with the AT_1 receptor. In fact, compounds **Id** and **Ie** displayed significantly higher affinity toward the AT_1 receptor than **Ic** and **If**, whereas compounds **Ia**, **Ib**, and **9** showed no affinity toward the same receptor. Optimal activity occurred with the linear valeryl chain (in **Id**), even though it is still in the micromolar affinity range. The relatively low AT_1 receptor affinity shown by the new compounds may be explained by a potential intramolecular hydrogen bonding interaction between the amide NH and the carbonyl function of the alkyl chain. The total loss of affinity shown by compound **9** indicates that not only the length of the side chain, but also its nature plays a key role in the affinity of these compounds toward the AT_1 receptor. Furthermore, shortening of the acyl chain of **Id** to butyryl, propanoyl, or acetyl gave rise to compounds of lower (**Ic**) or no affinity (**Ia** and **Ib**). Similarly, lengthening of the valeryl chain to hexanoyl or heptanoyl (respectively **Ie** and **If**) resulted in a slight decrease in affinity, which was more pronounced in compound **If**. In summary, on the basis of molecular modeling studies, we have designed a new series of chiral pyrrolidine-2-ylcarboxamides as AT_1 receptor ligands. In the future the effect of stereoselectivity will be studied in detail to determine if this new series of compounds binds to the AT_1 receptor in a stereoselective manner.

Experimental Section

General remarks: All chemicals were purchased from Sigma–Aldrich or Lancaster in the highest quality commercially available. Solvents were RP grade unless otherwise indicated. Yields refer to purified products and were not optimized. The structures of the compounds were confirmed by routine spectrometric analyses. Only spectra for compounds not previously described are given. The NH proton of the tetrazole is undetectable in ^{1}H NMR spectra. Melting points were determined on a Gallenkamp melting point apparatus in open glass capillary tubes and are uncorrected. The IR spectra were recorded on a PerkinElmer Spectrum One FT spectrophotometer (Norwalk, CT). ^{1}H NMR and ^{13}C NMR spectra were recorded on a Varian VX Mercury spectrometer, operating at 300 and 75 MHz for ^{1}H and ^{13}C NMR, respectively. Chemical shifts are reported relative to solvent resonance: $CDCl_3$, $\delta = 7.26$ ppm (^{1}H NMR) and $\delta = 77.3$ ppm (^{13}C NMR); [D_6]DMSO, $\delta = 2.50$ ppm (^{1}H NMR) and $\delta = 39.5$ ppm (^{13}C NMR); CD_3OD, $\delta = 47.8$ ppm (^{13}C NMR). GC–MS was performed on a Hewlett–Packard 6890–5973 MSD at low resolution. LC–MS was performed on an Agilent 1100 series LC–MSD Trap System VL spectrometer. Elemental analyses were within ± 0.4% of theoretical values and were performed on a Eurovector Euro EA 3000 analyzer. Chromatographic separations were performed on silica gel columns by flash chromatography (Kieselgel 60, 0.040–0.063 mm, Merck, Darmstadt, Germany) using the technique described by Still et al.[37] TLC analyses were performed on precoated silica gel on aluminum sheets (Kieselgel 60 F_{254}, Merck).

4′-(Bromomethyl)biphenyl-2-carbonitrile (2): *N*-Bromosuccinimide (2.11 g, 11.9 mmol) and benzoyl peroxide (0.20 g, 0.83 mmol) were added to a stirred solution of the commercially available 4′-methylbiphenyl-2-carbonitrile (**1**) (2.30 g, 11.9 mmol) in CCl_4 (70 mL). The reaction was held at reflux for 3 h. The solid residue was filtered off, and the filtrate was concentrated under vacuum; the residue was then purified by column chromatography (EtOAc/petroleum ether 1.5:8.5) to give a pale-yellow oil, which was crystallized from $CHCl_3$/hexane to give white crystals (2.10 g, 65%): mp: 125–126 °C (lit: 114.5–120.0 °C[9]); other spectroscopic data were in agreement with those reported.[9]

4′-[(1,3-Dioxo-1,3-dihydro-2*H*-isoindol-2-yl)methyl]biphenyl-2-carbonitrile (3): A stirred solution of compound **2** (3.0 g, 11.0 mmol) and potassium phthalimide (2.24 g, 12.0 mmol) in dry DMF (30 mL) was heated under nitrogen atmosphere at 130 °C for 7 h. The mixture was cooled, the solvent was removed under reduced pressure, and H_2O was added. The resulting suspension was extracted twice with $CHCl_3$, and the combined organic phases were dried (Na_2SO_4) and concentrated to give a white solid, which was recrystallized from $CHCl_3$/hexane to give white crystals (3.40 g, 91%): mp: 180–181 °C (lit: 150–153 °C (EtOAc)[38]); ^{1}H NMR ($CDCl_3$): $\delta = 4.91$ (s, 2H), 7.35–7.65 (m, 7H), 7.66–7.80 (m, 3H), 7.82–7.90 ppm (m, 2H); ^{13}C NMR ($CDCl_3$): $\delta = 41.5$ (1C), 111.4 (1C), 118.8 (1C), 123.7 (2C), 127.8 (1C), 129.3 (3C), 130.3 (1C), 132.3 (2C), 133.1 (2C), 134.0 (2C), 134.3 (2C), 137.1 (1C), 145.2 (1C), 168.3 ppm (2C); IR (KBr): $\tilde{\nu} = 2219$ (C≡N), 1770, 1713 cm^{-1} (C=O); GC–MS data are in agreement with those reported;[38] anal. calcd for $C_{22}H_{14}N_2O_2$ (338.36): C 78.09, H 4.17, N 8.28, found: C 78.03, H 4.32, N 8.00.

4′-(Aminomethyl)biphenyl-2-carbonitrile (4): Compound **3** (2.0 g, 5.91 mmol) was suspended in a mixture of absolute EtOH (15 mL) and CH_3OH (30 mL), and the resulting suspension was vigorously stirred. Then, 98% hydrazine hydrate (0.94 mL, 29.6 mmol) was added portion-wise to the solution. The mixture was heated at reflux for 1.5 h, and then the precipitate was filtered off; the filtrate was evaporated under vacuum. The residue was taken up with EtOAc and extracted twice with HCl (2 N); then the aqueous phase was made alkaline with NaOH (2 N) and extracted twice with EtOAc. The combined organic layers were dried (Na_2SO_4) and concentrated to give 1.09 g of a pale-yellow oil (88%): ^{1}H NMR ($CDCl_3$): $\delta = 1.84$ (br s, 2H, exch D_2O), 3.94 (br s, 2H), 7.35–7.55 (m, 6H), 7.55–7.65 (m, 1H), 7.70–7.80 ppm (m, 1H); ^{13}C NMR ($CDCl_3$): $\delta = 46.3$ (1C), 111.4 (1C), 119.0 (1C), 127.7 (1C), 128.9 (1C), 129.2 (2C), 130.2 (1C), 133.0 (1C), 134.0 (2C), 136.9 (1C), 143.9 (1C), 145.5 ppm (1C); IR (neat): $\tilde{\nu} = 3370$ (NH_2), 2223 cm^{-1} (C≡N); GC–MS (70 eV): *m/z* (%): 208 (100).

(*R*,*S*)-*tert*-Butyl-2-({[(2′-cyanobiphenyl-4-yl)methyl]amino}carbonyl)pyrrolidine-1-carboxylate (5): (*RS*)-1-(*tert*-butoxycarbonyl)pyrrolidine-2-carboxylic acid (0.94 g, 4.37 mmol), EEDQ (1.29 g, 5.22 mmol), and Et_3N (0.91 mL, 6.55 mmol) were added to a solution of **4** (1.0 g, 4.80 mmol) in $CHCl_3$ (130 mL). The reaction mixture was held at reflux for 24 h. The solvent was evaporated, and the residue was taken up with EtOAc and washed three times with HCl (2 N), three times with NaOH (2 N), and once with H_2O. The organic phase was dried (Na_2SO_4) and concentrated under vacuum. Purification of the residue by column chromatography (EtOAc/petroleum ether 8:2) and recrystallization from EtOAc/hexane gave white crystals (1.54 g, 87%): mp: 127–129 °C; ^{1}H NMR ($CDCl_3$): $\delta = 1.42$ (br s, 9H), 1.82–2.48 (m, 4H), 3.44 (br s, 2H), 4.40 (br d, $J = 50.9$ Hz, 3H), 6.48 (br s, 1H), 7.35–7.55 (m, 6H), 7.60–7.70 (m, 1H), 7.70–7.80 ppm (m, 1H); ^{13}C NMR ($CDCl_3$): $\delta = 24.9$ (1C), 28.6 (3C), 31.0 (1C), 43.2 (1C), 47.4 (1C), 60.5 (1C), 80.8 (1C), 111.4 (1C), 118.9 (1C), 127.8 (3C), 129.3 (1C), 130.2 (1C), 133.1 (1C), 134.0 (2C), 137.3 (1C), 139.2 (1C), 145.3 (1C), 155.0 (1C), 171.3 ppm (1C); IR (KBr): $\tilde{\nu} = 3312$ (NH), 2224 (C≡N), 1690, 1670 cm^{-1} (C=O); GC–MS (70 eV): *m/z* (%): 305 [$M^+ - 100$, < 1], 70 (100); anal. calcd for

$C_{24}H_{27}N_3O_3$ (405.49): C 71.09, H 6.71, N 10.36, found: C 71.31, H 6.71, N 10.41.

(*R*,*S*)-*N*-[(2′-Cyanobiphenyl-4-yl)methyl]pyrrolidine-2-carboxamide (6): HBr (48%, 8.8 mL) was added to a solution of compound **5** (2.0 g, 4.93 mmol) in EtOAc (30 mL). The mixture was stirred at room temperature for 4 h, then washed twice with H_2O. The combined aqueous layers were made alkaline with NaOH (2 N) and extracted twice with EtOAc. The organic phases were dried (Na_2SO_4) and concentrated to give a slightly yellowish oil (1.38 g, 92%): ^{1}H NMR ($CDCl_3$): δ = 1.60–1.85 (m, 2H), 1.85–2.05 (m, 1H, exch D_2O), 2.05–2.30 (m, 2H), 2.80–3.08 (m, 2H), 3.75–3.85 (m, 1H), 4.49 (d, J = 6.1 Hz, 2H), 7.30–7.55 (m, 6H), 7.55–7.65 (m, 1H), 7.70–7.80 (m, 1H), 8.08 ppm (br s, 1H, exch D_2O); ^{13}C NMR ($CDCl_3$): δ = 26.5 (1C), 31.1 (1C), 42.8 (1C), 47.5 (1C), 60.8 (1C), 111.4 (1C), 118.9 (1C), 127.8 (2C), 128.1 (1C), 129.2 (1C), 130.2 (1C), 133.1 (1C), 134.0 (2C), 137.3 (1C), 139.6 (1C), 145.3 (1C), 175.5 ppm (1C); IR (neat): $\tilde{\nu}$ = 3324 (NH), 2223 (C≡N), 1660 cm^{-1} (C=O); GC–MS (70 eV): *m/z* (%): 305 [M^+, < 1], 70 (100).

(*R*,*S*)-1-Acetyl-*N*-[(2′-cyanobiphenyl-4-yl)methyl]pyrrolidine-2-carboxamide (7a): A solution of **6** (1.29 g, 4.22 mmol) and Et_3N (0.88 mL, 6.33 mmol) in toluene (150 mL) was stirred and brought to reflux; acetyl chloride (0.93 g, 11.9 mmol) was then added, and the reaction was held at reflux for 24 h. The solvent was evaporated, and the residue, dissolved in $CHCl_3$, was washed three times with HCl (2 N) and once with H_2O. The organic layer was dried (Na_2SO_4) and concentrated under reduced pressure. Purification of the residue by crystallization from $CHCl_3$/hexane gave white crystals (1.07 g, 73%): mp: 154–155 °C; ^{1}H NMR ($CDCl_3$): δ = 1.75–1.93 (m, 2H), 1.95–2.05 (m, 1H), 2.10 (s, 3H), 2.42–2.52 (m, 1H), 3.37–3.48 (m, 1H), 3.52–3.62 (m, 1H), 4.37–4.54 (m, 2H), 4.57–4.65 (m, 1H), 7.33–7.40 (m, 2H), 7.40–7.53 (m, 4H), 7.56–7.66 (m 2H), 7.71–7.78 ppm (m, 1H); ^{13}C NMR ($CDCl_3$): δ = 22.8 (1C), 25.3 (1C), 27.7 (1C), 43.3 (1C), 48.6 (1C), 59.9 (1C), 111.4 (1C), 119.0 (1C), 127.7 (2C), 128.0 (1C), 129.2 (1C), 130.3 (1C), 133.1 (1C), 134.0 (2C), 137.2 (1C), 139.4 (1C), 145.4 (1C), 171.4 (1C), 171.3 ppm (1C); IR (KBr): $\tilde{\nu}$ = 3291 (NH), 2227 (C≡N), 1665, 1630 cm^{-1} (C=O); GC–MS (70 eV): *m/z* (%): 347 [M^+, 10], 70 (100); anal. calcd for $C_{21}H_{21}N_3O_2 \cdot 0.66\ H_2O$ (359.41): C 70.18, H 6.26, N 11.69, found: C 70.18, H 6.00 N 11.62.

(*R*,*S*)-*N*-[(2′-Cyanobiphenyl-4-yl)methyl]-1-propionylpyrrolidine-2-carboxamide (7b): Propionic acid (0.32 mL, 4.27 mmol), EEDQ (1.27 g, 5.12 mmol), and Et_3N (0.89 mL, 6.40 mmol) were added to a stirred solution of **6** (1.43 g, 4.70 mmol) in $CHCl_3$ (180 mL). The reaction mixture was held at reflux for 24 h. The solvent was evaporated, and the residue was taken up with EtOAc and washed three times with HCl (2 N), three times with NaOH (2 N), and once with H_2O. The organic phase was dried (Na_2SO_4) and concentrated under vacuum. Purification of the residue by flash chromatography (EtOAc) gave white crystals (0.99 g, 64%), which were recrystallized from EtOAc: mp: 153–154 °C; ^{1}H NMR ($CDCl_3$): δ = 1.07 (t, J = 7.5 Hz, 3H), 1.76–1.90 (m, 2H), 1.92–2.22 (m, 1H), 2.34 (q, J = 7.3 Hz, 2H), 2.41–2.51 (m, 1H), 3.35–3.46 (m, 1H), 3.48–3.61 (m, 1H), 4.38–4.54 (m, 2H), 4.60–4.68 (m, 1H), 7.32–7.53 (m, 6H), 7.52–7.70 (m, 2H), 7.70–7.78 ppm (m, 1H); ^{13}C NMR ($CDCl_3$): δ = 9.1 (1C), 25.3 (1C), 27.4 (1C), 28.1 (1C), 43.2 (1C), 47.6 (1C), 60.0 (1C), 111.4 (1C), 119.0 (1C), 127.7 (2C), 128.0 (1C), 129.2 (1C), 130.3 (1C), 133.1 (1C), 134.0 (2C), 137.2 (1C), 139.5 (1C), 145.4 (1C), 171.7 (1C), 174.6 ppm (1C); IR (KBr): $\tilde{\nu}$ = 3292 (NH), 2221 (C≡N), 1683, 1632 cm^{-1} (C=O); GC–MS (70 eV): *m/z* (%): 361 [M^+, 8], 70 (100); anal. calcd for $C_{22}H_{23}N_3O_2$ (361.44): C 73.11, H 6.41, N 11.63, found: C 72.88, H 6.38, N 11.58.

(*R*,*S*)-1-Butyryl-*N*-[(2′-cyanobiphenyl-4-yl)methyl]pyrrolidine-2-carboxamide (7c): Compound **7c** was synthesized (52%) using the procedure described for **7b** starting from **6** and butyric acid. White solid: mp: 151–152 °C; ^{1}H NMR ($CDCl_3$): δ = 0.87 (t, J = 7.4 Hz, 3H), 1.66 (apparent sextet, J = 7.4 Hz, 2H), 1.72–1.90 (m, 1H), 1.92–2.20 (m, 2H), 2.30 (t, J = 7.3 Hz, 2H), 2.42–2.56 (m, 1H), 3.36–3.48 (m, 1H), 3.51–3.63 (m, 1H), 4.34–4.54 (m, 2H), 4.65 (d, J = 6.9 Hz, 1H), 7.32–7.54 (m, 6H), 7.58–7.70 (m, 2H), 7.72–7.80 ppm (m, 1H); ^{13}C NMR ($CDCl_3$): δ = 14.1 (1C), 18.4 (1C), 25.3 (1C), 27.3 (1C), 36.7 (1C), 43.2 (1C), 47.8 (1C), 59.9 (1C), 111.4 (1C), 118.9 (1C), 127.7 (2C), 128.0 (1C), 129.2 (1C), 130.3 (1C), 133.1 (1C), 134.0 (2C), 137.2 (1C), 139.4 (1C), 145.4 (1C), 171.6 (1C), 174.0 ppm (1C); IR (KBr): $\tilde{\nu}$ = 3294 (NH), 2220 (C≡N), 1684, 1630 cm^{-1} (C=O); GC–MS (70 eV): *m/z* (%): 375 [M^+, 5], 70 (100); anal. calcd for $C_{23}H_{25}N_3O_2 \cdot 0.80\ H_2O$ (389.86): C 70.85, H 6.88, N 10.78, found: C 70.96, H 6.63, N 10.37.

(*R*,*S*)-*N*-[(2′-Cyanobiphenyl-4-yl)methyl]-1-pentanoylpyrrolidine-2-carboxamide (7d): Compound **7d** was synthesized (67%) using the procedure described for **7b** starting from **6** and valeric acid. Pale-yellow oil: ^{1}H NMR ($CDCl_3$): δ = 0.89 (t, J = 7.3 Hz, 3H), 1.38–1.42 (m, 2H), 1.50–1.58 (m, 2H), 1.75–2.20 (m, 3H), 2.32 (t, J = 7.6 Hz, 2H), 2.40–2.52 (m, 1H), 3.35–3.50 (m, 1H), 3.50–3.65 (m, 1H), 4.35–4.55 (m, 2H), 4.60–4.70 (m, 1H), 7.32–7.54 (m, 6H), 7.58–7.68 (m, 2H), 7.70–7.78 ppm (m, 1H); ^{13}C NMR ($CDCl_3$): δ = 14.1 (1C), 22.7 (1C), 25.3 (1C), 27.1 (1C), 27.4 (1C), 34.6 (1C), 43.2 (1C), 47.8 (1C), 59.9 (1C), 111.4 (1C), 119.0 (1C), 127.7 (2C), 128.0 (1C), 129.2 (1C), 130.3 (1C), 133.1 (1C), 134.0 (2C), 137.2 (1C), 139.4 (1C), 145.4 (1C), 171.7 (1C), 174.1 ppm (1C); IR (neat): $\tilde{\nu}$ = 3294 (NH), 2223 (C≡N), 1631 cm^{-1} (C=O); GC–MS (70 eV): *m/z* (%): 389 [M^+, 4], 70 (100).

(*R*,*S*)-*N*-[(2′-Cyanobiphenyl-4-yl)methyl]-1-hexanoylpyrrolidine-2-carboxamide (7e): A solution of **6** (1.20 g, 3.93 mmol) and Et_3N (1.15 mL, 8.26 mmol) in anhydrous THF (150 mL) was stirred and brought to reflux under nitrogen atmosphere; then hexanoyl chloride (1.48 g, 11.0 mmol), obtained by treatment of hexanoic acid with $SOCl_2$, was added, and the reaction was held at reflux for 7 h. The solid was filtered off, and the solvent was evaporated under reduced pressure. The residue, dissolved in ethyl acetate, was washed twice with HCl (2 N) and once with NaOH (2 N). The organic layer was dried (Na_2SO_4) and concentrated under reduced pressure. Purification of the residue by column chromatography (EtOAc) and recrystallization from EtOAc gave white crystals (1.10 g, 69%): mp: 119–120 °C (EtOAc); ^{1}H NMR ($CDCl_3$): δ = 0.86 (t, J = 6.7 Hz, 3H), 1.22–1.36 (m, 4H), 1.52–1.60 (m, 2H), 1.75–2.20 (m, 3H), 2.30 (t, J = 7.6 Hz, 2H), 2.38–2.52 (m, 1H), 3.36–3.48 (m, 1H), 3.52–3.62 (m, 1H), 4.35–4.53 (m, 2H), 4.62 (d, J = 7.1 Hz, 1H), 7.32–7.52 (m, 6H), 7.57–7.77 ppm (m, 3H); ^{13}C NMR ($CDCl_3$): δ = 14.2 (1C), 22.7 (1C), 24.7 (1C), 25.3 (1C), 27.4 (1C), 31.8 (1C), 34.8 (1C), 43.2 (1C), 47.8 (1C), 59.9 (1C), 111.4 (1C), 118.9 (1C), 127.7 (2C), 127.9 (1C), 129.2 (1C), 130.2 (1C), 133.1 (1C), 134.0 (2C), 137.2 (1C), 139.4 (1C), 145.4 (1C), 171.7 (1C), 174.1 ppm (1C); IR (KBr): $\tilde{\nu}$ = 3315 (NH), 2215 (C≡N), 1663, 1627 cm^{-1} (C=O); GC–MS (70 eV): *m/z* (%): 403 [M^+, 6], 70 (100); anal. calcd for $C_{25}H_{29}N_3O_2$ (403.52): C 74.41, H 7.24, N 10.41, found: C 74.25, H 7.37, N 10.11.

(*R*,*S*)-*N*-[(2′-Cyanobiphenyl-4-yl)methyl]-1-heptanoylpyrrolidine-2-carboxamide (7f): Compound **7f** was synthesized (56%) using the procedure described for **7e** starting from **6** and heptanoyl chloride. White crystals: mp: 108–110 °C (EtOAc); ^{1}H NMR ($CDCl_3$): δ = 0.84 (t, J = 6.5 Hz, 3H), 1.18–1.38 (m, 6H), 1.55–1.68 (m, 2H), 1.76–2.20 (m, 3H), 2.31 (t, J = 7.6 Hz, 2H), 2.41–2.52 (m, 1H), 3.36–3.48 (m, 1H), 3.51–3.62 (m, 1H), 4.34–4.56 (m, 2H), 4.64 (dd, J = 8.0, 1.6 Hz, 1H), 7.32–7.53 (m, 6H), 7.57–7.76 ppm (m, 3H); ^{13}C NMR

($CDCl_3$): $\delta = 14.2$ (1C), 22.7 (1C), 25.0 (1C), 25.3 (1C), 27.4 (1C), 29.3 (1C), 31.8 (1C), 34.9 (1C), 43.2 (1C), 47.8 (1C), 59.9 (1C), 111.4 (1C), 118.9 (1C), 127.7 (2C), 127.9 (1C), 129.2 (1C), 130.2 (1C), 133.0 (1C), 134.0 (2C), 137.2 (1C), 139.5 (1C), 145.4 (1C), 171.7 (1C), 174.1 ppm (1C); IR (KBr): $\tilde{\nu} = 3314$ (NH), 2214 (C≡N), 1664, 1616 cm^{-1} (C=O); GC–MS (70 eV): *m/z* (%): 417 [M^+, 4], 70 (100); anal. calcd for $C_{26}H_{31}N_3O_2$ (417.54): C 74.79, H 7.48, N 10.06, found: C 75.05, H 7.55, N 10.11.

(*R*,*S*)-1-Acetyl-*N*-({2′-[1-(trimethylstannyl)-1*H*-tetrazol-5-yl]biphenyl-4-yl}methyl)pyrrolidine-2-carboxamide (8a): A solution of compound **7a** (0.55 g, 1.58 mmol) in dry toluene (10 mL) and azidotrimethyltin (0.62 g, 3.01 mmol) was kept at 110 °C under nitrogen atmosphere for 48 h. The precipitate was filtered off and washed with hot toluene to give **8a** as a brown solid (0.85 mg, 97%): mp: > 250 °C; IR (KBr): $\tilde{\nu} = 1628$ (C=O), 551 cm^{-1} (Sn-N); LC–MS *m/z* (%): 389 [$M^+ - 165$]; the presence of the trimethyltin group was assured by ^1H NMR ([D_6]DMSO) $\delta = 0.90$ ppm.

(*R*,*S*)-1-Propionyl-*N*-({2′-[1-(trimethylstannyl)-1*H*-tetrazol-5-yl]biphenyl-4-yl}methyl)pyrrolidine-2-carboxamide (8b): Compound **8b** was synthesized (76%) using the same procedure described for **8a** starting from **7b**. White solid: mp: > 250 °C (toluene); IR (KBr): $\tilde{\nu} = 1691$, 1613 (C=O), 545 cm^{-1} (Sn–N); LC–MS *m/z* (%): 591 [$M^+ + 23$].

(*R*,*S*)-1-Butyryl-*N*-({2′-[1-(trimethylstannyl)-1*H*-tetrazol-5-yl]biphenyl-4-yl}methyl)pyrrolidine-2-carboxamide (8c): Compound **8c** was synthesized (95%) using the same procedure described for **8a** starting from **7c**. Beige solid: mp: > 250 °C (toluene); IR (KBr): $\tilde{\nu} = 1691$, 1626 (C=O), 546 cm^{-1} (Sn–N); LC–MS *m/z* (%): 605 [$M^+ + 23$].

(*R*,*S*)-1-Pentanoyl-*N*-({2′-[1-(trimethylstannyl)-1*H*-tetrazol-5-yl]biphenyl-4-yl}methyl)pyrrolidine-2-carboxamide (8d): Compound **8d** was synthesized (96%) using the same procedure described for **8a** starting from **7d**. Brown solid: mp: > 250 °C (toluene); IR (KBr): $\tilde{\nu} = 1691$, 1626 (C=O), 546 cm^{-1} (Sn–N); LC–MS *m/z* (%): 619 [$M^+ + 23$].

(*R*,*S*)-1-Hexanoyl-*N*-({2′-[1-(trimethylstannyl)-1*H*-tetrazol-5-yl]biphenyl-4-yl}methyl)pyrrolidine-2-carboxamide (8e): Compound **8e** was synthesized (76%) using the same procedure described for **8a** starting from **7e**. Brown oil: IR (neat): $\tilde{\nu} = 1629$ (C=O), 549 cm^{-1} (Sn–N); LC–MS *m/z* (%): 631 [$M^+ + 23$].

(*R*,*S*)-1-Heptanoyl-*N*-({2′-[1-(trimethylstannyl)-1*H*-tetrazol-5-yl]biphenyl-4-yl}methyl)pyrrolidine-2-carboxamide (8e): Compound **8f** was synthesized (76%) using the same procedure described for **8a** starting from **7f**. Brown oil: IR (neat): $\tilde{\nu} = 1633$ (C=O), 550 cm^{-1} (Sn–N). LC–MS *m/z* (%): 645 [$M^+ + 23$].

(*R*,*S*)-1-Acetyl-*N*-{[2′-(1*H*-tetrazol-5-yl)biphenyl-4-yl]methyl}pyrrolidine-2-carboxamide (Ia): Compound **Ia** was directly obtained (39%) by column chromatography (EtOAc/EtOH 9:1) of **8a**. Beige solid: mp: 179–181 °C; ^1H NMR ([D_6]DMSO): $\delta = 1.70$–2.05 (m overlapping s at 1.96, 4H), 1.96 (s overlapping m at 1.70–2.05, 3H), 3.25–3.60 (m, 3H), 4.20–4.38 (m, 2H), 6.95–7.05 (m, 2H), 7.12–7.20 (m, 2H), 7.48–7.60 (m, 2H), 7.60–7.72 (m, 2H), 8.33 ppm (apparent t, $J = 6.0$ Hz, 1H); ^{13}C NMR ([D_6]DMSO): $\delta = 19.4$ (1C), 21.3 (1C), 26.8 (1C), 38.4 (1C), 44.5 (1C), 56.5 (1C), 120.4 (1C), 123.6 (1C), 124.0 (2C), 124.6 (1C), 125.6 (1C), 127.6 (2C), 128.1 (1C), 134.5 (1C), 135.9 (1C), 138.3 (1C), 152.0 (1C), 165.7 (1C), 169.0 ppm (1C); IR (KBr): $\tilde{\nu} = 1627$ (C=O) cm^{-1}; IR (KBr): $\tilde{\nu} = 3294$ (NH), 1668, 1644 cm^{-1} (C=O); LC–MS *m/z* (%): 389 [$M^+ - 1$]; anal. calcd for $C_{21}H_{22}N_6O_2 \cdot 0.75\,C_2H_5OH$ (424.99): C 63.59, H 6.28, N 19.77, found: C 63.57, H 6.04, N 19.50.

(*R*,*S*)-1-Propionyl-*N*-{[2′-(1*H*-tetrazol-5-yl)biphenyl-4-yl]methyl}pyrrolidine-2-carboxamide (Ib): A suspension of compound **8b** (0.60 g, 1.06 mmol) in a mixture of toluene (8 mL) and THF (2 mL) was stirred in an ice bath. Gaseous HCl was then added to give a clear solution followed by precipitation of the desired product. The precipitate was filtered, and the filtrate was washed with toluene and purified by crystallization from MeOH/Et_2O to give a brown solid (0.39 g, 91%): mp: 182–183 °C; ^1H NMR ([D_6]DMSO): $\delta = 0.95$ (t, $J = 7.3$ Hz, 3H), 1.68–2.35 (m, 6H), 3.22–3.60 (m, 3H), 4.18–4.36 (m, 2H), 6.95–7.05 (m, 2H), 7.10–7.20 (m, 2H), 7.46–7.72 (m, 4H), 8.29 ppm (apparent t, $J = 5.8$ Hz, 1H); ^{13}C NMR (CD_3OD): $\delta = 8.0$ (1C), 24.5 (1C), 27.2 (1C), 27.3 (1C), 42.3 (1C), 47.4 (1C), 60.5 (1C), 123.1 (1C), 127.2 (1C), 127.6 (2C), 127.7 (1C), 129.0 (1C), 130.5 (2C), 131.4 (1C), 138.2 (1C), 138.6 (1C), 142.1 (1C), 155.5 (1C), 173.9 (1C), 174.4 ppm (1C); IR (KBr): $\tilde{\nu} = 3388$ (NH), 1627 cm^{-1} (C=O); LC–MS *m/z* (%): 403 [$M^+ - 1$]; anal. calcd for $C_{22}H_{24}N_6O_2 \cdot 0.50\,H_2O \cdot 0.50\,CH_3OH$ (429.49): C 62.92, H 6.34, N 19.57, found: C 62.80, H 6.02, N 19.35.

(*R*,*S*)-1-Butyryl-*N*-{[2′-(1*H*-tetrazol-5-yl)biphenyl-4-yl]methyl}pyrrolidine-2-carboxamide (Ic): Compound **Ic** was synthesized (42%) using the same procedure described for **Ib** starting from **8c**. Beige solid: mp: 136–137 °C (EtOH/Et_2O); ^1H NMR ([D_6]DMSO): $\delta = 0.82$ (apparent dt, $J = 31.2$, 7.3 Hz, 3H), 1.36–1.58 (m, 2H), 1.69–2.32 (m 6H), 3.18–3.66 (m, 3H), 4.16–4.40 (m, 2H), 6.95–7.05 (m, 2H), 7.16 (apparent d, $J = 7.8$ Hz, 2H), 7.45–7.72 (m, 4H), 8.29 ppm (apparent t, $J = 5.8$ Hz, 1H); ^{13}C NMR ([D_6]DMSO): $\delta = 14.5$ (1C), 18.3 (1C), 25.0 (1C), 30.2 (1C), 36.2 (1C), 42.1 (1C), 47.4 (1C), 60.2 (1C), 124.1 (1C), 127.3 (1C), 127.6 (2C), 128.3 (1C), 129.3 (1C), 131.3 (2C), 131.8 (1C), 138.2 (1C), 139.6 (1C), 142.0 (1C), 155.5 (1C), 171.6 (1C), 172.7 ppm (1C); IR (KBr): $\tilde{\nu} = 3415$ (NH), 1624 cm^{-1} (C=O); LC–MS *m/z* (%): 417 [$M^+ - 1$]; anal. calcd for $C_{23}H_{26}N_6O_2 \cdot 1.50\,H_2O$ (445.49): C 62.01, H 6.56, N 18.86, found: C 62.01, H 6.19, N 18.51.

(*R*,*S*)-1-Pentanoyl-*N*-{[2′-(1*H*-tetrazol-5-yl)biphenyl-4-yl]methyl}pyrrolidine-2-carboxamide (Id): Compound **Id** was synthesized (42%) using the same procedure described for **Ib** starting from **8c**. Tan solid: mp: 146–147 °C (EtOH/Et_2O); ^1H NMR ([D_6]DMSO): $\delta = 0.82$ (apparent dt, $J = 20.5$, 7.3 Hz, 3H), 1.08–1.52 (m, 4H), 1.68–2.37 (m, 6H), 3.29–3.45 (m, 3H), 4.18–4.42 (m, 2H), 6.95–7.08 (m, 2H), 7.15 (apparent d, $J = 7.8$ Hz, 2H), 7.45–7.72 (m, 4H), 8.30 ppm (apparent t, $J = 5.8$ Hz, 1H); ^{13}C NMR ([D_6]DMSO): $\delta = 14.6$ (1C), 22.6 (1C), 25.0 (1C), 27.0 (1C), 30.2 (1C), 32.5 (1C), 42.0 (1C), 47.4 (1C), 60.2 (1C), 124.1 (1C), 127.3 (1C), 127.6 (2C), 128.3 (1C), 129.3 (1C), 131.3 (2C), 131.8 (1C), 138.2 (1C), 139.6 (1C), 142.0 (1C), 154.9 (1C), 171.7 (1C), 172.7 ppm (1C); IR (KBr): $\nu\ddot{U} = > = 3402$ (NH), 1626 cm^{-1} (C=O); LC–MS *m/z* (%): 431 [$M^+ - 1$]; anal. calcd for $C_{24}H_{28}N_6O_2 \cdot 0.50\,C_2H_5OH \cdot 0.50\,H_2O$ (464.55): C 64.63, H 6.94, N 18.09, found: C 64.18, H 6.55, N 18.09.

(*R*,*S*)-1-Hexanoyl-*N*-{[2′-(1*H*-tetrazol-5-yl)biphenyl-4-yl]methyl}pyrrolidine-2-carboxamide (Ie): Compound **Ie** was synthesized (70%) using the same procedure described for **Ib** starting from **8e.** Pale yellow solid: mp: 176–178 °C (EtOH/Et_2O); ^1H NMR ([D_6]DMSO): $\delta = 0.72$–0.90 (m, 3H), 1.1–1.57 (m, 6H), 1.68–2.35 (m, 4H), 3.3–3.75 (m, 5H), 4.15–4.45 (m, 2H), 6.95–7.1 (m, 4H), 7.25–7.60 (m, 4H), 8.30 ppm (apparent t, $J = 5.6$ Hz, 1H); ^{13}C NMR ([D_6]DMSO): $\delta = 14.5$ (1C), 22.7 (1C), 24.5 (1C), 25.0 (1C), 30.2 (1C), 31.7 (1C), 32.5 (1C), 42.2 (1C), 47.4 (1C), 60.2 (1C), 126.7 (1C), 127.0 (1C), 127.3 (2C), 128.4 (1C), 129.6 (1C), 130.7 (2C), 131.2 (1C), 138.1 (1C), 140.7 (1C), 141.1 (1C), 160.7 (1C), 171.7 (1C), 172.7 ppm (1C); IR (KBr): $\tilde{\nu} = 3456$ (NH), 1634 cm^{-1} (C=O); LC–MS *m/z* (%): 445 [$M^+ - 1$]; anal. calcd for $C_{25}H_{30}N_6O_2 \cdot H_2O$ (464.56): C 64.63, H 6.94, N 18.09, found: C 64.75, H 6.58, N 18.14.

(*R*,*S*)-1-Heptanoyl-*N*-{[2′-(1*H*-tetrazol-5-yl)biphenyl-4-yl]methyl}-pyrrolidine-2-carboxamide (If): Compound **If** was synthesized (24%) using the same procedure described for **Ib** starting from **8f.** Tan solid: mp: 174–176 °C (EtOH/Et_2O); ^{1}H NMR ([D_6]DMSO): δ = 0.72–0.93 (m, 3H), 1.08–1.62 (m, 8H), 1.58–2.35 (m, 4H), 3.12–3.62 (m, 5H), 4.18–4.36 (m, 2H), 7.00 (apparent d, J = 8.0 Hz, 2H), 7.14 (apparent d, J = 8.0 Hz, 2H), 7.40–7.75 (m, 4H), 8.28 ppm (apparent t, J = 5.9 Hz, 1H); ^{13}C NMR (CD_3OD): δ = 13.2 (1C), 22.4 (1C), 24.6 (1C), 28.9 (1C), 29.8 (1C), 31.6 (1C), 32.1 (1C), 34.3 (1C), 42.4 (1C), 47.6 (1C), 60.5 (1C), 123.5 (1C), 127.2 (1C), 127.5 (2C), 127.7 (1C), 129.1 (1C), 130.7 (2C), 131.2 (1C), 138.5 (1C), 139.6 (1C), 142.1 (1C), 155.9 (1C), 173.4 (1C), 173.8 ppm (1C); IR (KBr): $\tilde{\nu}$ = 3449 (NH), 1630 cm^{-1} (C=O); LC–MS *m/z* (%): 459 [M^+ −1]; anal. calcd for $C_{26}H_{32}N_6O_2 \cdot 1.50\,H_2O$ (487.57): C 64.04, H 7.24, N 17.24, found: C 64.32, H 7.04, N 17.53.

(*R*,*S*)-*tert*-Butyl-2-[({[2′-(1*H*-tetrazol-5-yl)biphenyl-4-yl]methyl}amino)carbonyl]pyrrolidine-1-carboxylate (9): Compound **9**, as an oil, was synthesized using the same procedure described for **8a** starting from **5** followed by column chromatography (EtOAc as eluent). The colorless oil was recrystallized from EtOH/Et_2O to give white crystals (88%): mp: 158–160 °C; ^{1}H NMR ([D_6]DMSO): δ = 1.26 (s, 6H), 1.38 (s, 3H), 1.70–1.85 (m, 3H), 2.0–2.10 (m, 1H), 3.32 (br s, 2H), 4.0–4.25 (m, 2H), 4.25–4.40 (m, 1H), 6.95–7.05 (m, 2H), 7.12–7.20 (m, 2H), 7.45–7.58 (m, 2H), 7.60–7.72 (m, 2H), 8.30–8.45 ppm (m, 1H); ^{13}C NMR ([D_6]DMSO): δ = 23.8 (1C), 28.7 (3C), 30.6 (1C), 42.3 (1C), 47.2 (1C), 60.6 (1C), 79.2 (1C), 124.2 (1C), 128.2 (1C), 129.5 (2C), 130.1 (1C), 130.9 (1C), 131.5 (2C), 132.0 (1C), 138.4 (1C), 139.5 (1C), 142.0 (1C), 154.2 (1C), 155.8 (1C), 173.1 ppm (1C); IR (KBr): $\tilde{\nu}$ = 3294 (NH), 1668, 1644 cm^{-1} (C=O); LC–MS *m/z* (%): 447 [M^+ −1]; anal. calcd for $C_{24}H_{28}N_6O_3 \cdot 0.50\,C_2H_5OH$ (471.55): C 63.68, H 6.63, N 17.82, found: C 63.56, H 6.48, N 17.51.

Acknowledgements

This work was accomplished thanks to the financial support of the Ministero dell'Istruzione, dell'Università e della Ricerca (MIUR 2003033405). [^{3}H]Valsartan was kindly provided by Dr. M. de Gasparo (Novartis, Basel, Switzerland). P.V. is the holder of a Vrije Universiteit Brussel research fellowship. The authors thank Professor Cruciani for his valuable suggestions and critical reading of the manuscript. Thanks are also due to Professor Lentini for helpful input in the early stages of the project.

Keywords: amides · AT_1 receptors · hypertension · nitrogen heterocycles

[1] M. Moser, *Arch. Intern. Med.* **2001**, *161*, 1140 – 1144.
[2] "International Union of Pharmacology, XXIII. The Angiotensin II Receptors": M. De Gasparo, K. J. Catt, T. Inagami, J. W. Wright, T. Unger, *Pharmacol. Rev.* **2000**, *52*, 415 – 472.
[3] P. B. M. W. M. Timmermans, P. C. Wong, A. T. Chiu, W. F. Herblin, P. Benfield, D. J. Carini, R. J. Lee, R. R. Wexler, J. A. M. Saye, R. D. Smith, *Pharmacol. Rev.* **1993**, *45*, 205 – 251.
[4] J. R. Cockcroft, D. G. Sciberras, M. R. Goldberg, M. J. Ritter, *J. Cardiovasc. Pharmacol.* **1993**, *22*, 579 – 584.
[5] T. J. Murphy, R. W. Alexander, K. K. Griendling, M. S. Runge, K. E. Bernstein, *Nature* **1991**, *351*, 233 – 236.
[6] Y. Kambayashi, S. Bardhan, K. Takahashi, S. Tsuzuki, H. Inui, T. Hamakubo, T. Inagami, *J. Biol. Chem.* **1993**, *268*, 24543 – 24546.
[7] K. Sasaki, Y. Yamano, S. Bardhan, N. Iwai, J. J. Murray, M. Hasegawa, Y. Matsuda, T. Inagami, *Nature* **1991**, *351*, 230 – 233.
[8] U. M. Steckelings, E. Kaschina, T. Unger, *Peptides* **2005**, *26*, 1401 – 1409.
[9] D. J. Carini, J. V. Duncia, P. E. Aldrich, A. T. Chiu, A. L. Johnson, M. E. Pierce, W. A. Price, J. B. Santella III, G. J. Wells, R. R. Wexler, P. C. Wong, S.-E. Yoo, P. B. M. W. M. Timmermans, *J. Med. Chem.* **1991**, *34*, 2525 – 2547.
[10] R. R. Wexler, W. J. Greenlee, J. D. Irvin, M. R. Goldberg, K. Prendergast, R. D. Smith, P. B. M. W. M. Timmermans, *J. Med. Chem.* **1996**, *39*, 625 – 656.
[11] E. M. Krovat, T. Langer, *J. Med. Chem.* **2003**, *46*, 716 – 726.
[12] A. A. Boucard, B. C. Wilkes, S. A. Laporte, E. Escher, G. Guillemette, R. Leduc, *Biochemistry* **2000**, *39*, 9662 – 9670.
[13] S.-E. Yoo, S.-K. Kim, S.-H. Lee, N.-J. Kim, D. W. Lee, *Bioorg. Med. Chem.* **2000**, *8*, 2311 – 2316.
[14] A. Kurup, R. Garg, D. J. Carini, C. Hansch, *Chem. Rev.* **2001**, *101*, 2727 – 2750.
[15] T. Pandya, S. K. Pandey, M. Tiwari, S. C. Chaturvedi, A. K. Saxena, *Bioorg. Med. Chem.* **2001**, *9*, 291 – 300.
[16] K. Noda, Y. Saad, A. Kinoshita, T. P. Boyle, R. M. Graham, A. Husain, S. S. Karnik, *J. Biol. Chem.* **1995**, *270*, 2284 – 2289.
[17] B. Wilkes, L. Masaro, P. W. Schiller, K. A. Carpenter, *J. Med. Chem.* **2002**, *45*, 4410 – 4418.
[18] D. J. Underwood, C. D. Strader, R. Rivero, A. A. Patchett, W. Greenlee, K. Prendergast, *Chem. Biol.* **1994**, *1*, 211 – 221.
[19] S. Sciabola, I. Morao, M. J. De Groot, *J. Chem. Inf. Comput. Sci.* **2007**, *47*, 76 – 84.
[20] P. Bühlmayer, P. Furet, L. Criscione, M. de Gasparo, S. Whitebread, T. Schmidlin, R. Lattmann, J. Wood, *Bioorg. Med. Chem. Lett.* **1994**, *4*, 29 – 34.
[21] G. Berellini, G. Cruciani, R. Mannhold, *J. Med. Chem.* **2005**, *48*, 4389 – 4399.
[22] S.-E. Yoo, S.-K. Kim, S.-H. Lee, K. Y. Yi, D.-W. Lee, *Bioorg. Med. Chem.* **1999**, *7*, 2971 – 2976.
[23] B. Le Bourdonnec, E. Meulon, S. Yous, J.-F. Goossens, R. Houssin, J.-P. Hénichart, *J. Med. Chem.* **2000**, *43*, 2685 – 2697.
[24] SYBYL 6.5, Tripos Inc., 1699 South Hanley Road, St. Louis, MO 63144 (USA).
[25] M. Baroni, G. Costantino, G. Cruciani, D. Riganelli, R. Valigi, S. Clementi, *Quant.-Struct. Act. Relat.* **1993**, *12*, 9 – 20.
[26] G. Cruciani, P. Crivori, P.-A. Carrupt, B. Testa, *J. Mol. Struct. (THEOCHEM)* **2000**, *503*, 17 – 30.
[27] M. Pastor, G. Cruciani, I. McLay, S. Pickett, S. Clementi, *J. Med. Chem.* **2000**, *43*, 3233 – 3243.
[28] *Maybridge Chemicals Database*, Maybridge Chemicals Co. Ltd., Trevillet, Tintangel, Cornwall PL34 OHW (UK).
[29] P. M. L. Vanderheyden, F. L. P. Fierens, J. P. De Backer, N. Fraeyman, G. Vauquelin, *Br. J. Pharmacol.* **1999**, *126*, 1057 – 1065.
[30] I. Verheijen, F. L. P. Fierens, J. P. DeBacker, G. Vauquelin, P. M. L. Vanderheyden, *Fundam. Clin. Pharmacol.* **2000**, *14*, 577 – 585.
[31] E. Roubini, R. Laufer, C. Gilon, Z. Selinger, B. P. Roques, M. Chorev, *J. Med. Chem.* **1991**, *34*, 2430 – 2438.
[32] C. Franchini, F. Chiaia Noja, F. Corbo, G. Lentini, V. Tortorella, A. Bartolini, C. Ghelardini, R. Matucci, A. Giotti, *Chirality* **1993**, *5*, 135 – 142.
[33] M. A. Barton, R. U. Lemieux, J. Y. Savoie, *J. Am. Chem. Soc.* **1973**, *95*, 4501 – 4506.
[34] N. Izumiya, M. Muraoka, *J. Am. Chem. Soc.* **1969**, *91*, 2391 – 2392.
[35] J. V. Duncia, M. E. Pierce, J. B. Santella III, *J. Org. Chem.* **1991**, *56*, 2395 – 2400.
[36] W. T. Ashton, C. L. Cantone, L. L. Chang, S. M. Hutchins, R. A. Strelitz, M. MacCoss, R. S. L. Chang, V. J. Lotti, K. A. Faust, T.-B. Chen, P. Bunting, T. W. Schorn, S. D. Kivlighn, P. K. S. Siegl, *J. Med. Chem.* **1993**, *36*, 591 – 609.
[37] W. C. Still, M. Kahn, A. Mitra, *J. Org. Chem.* **1978**, *43*, 2923 – 2925.
[38] W. V. Murray, M. P. Wachter, US Patent 5182288, **1993**.

Received: April 11, 2007
Revised: June 1, 2007
Published online on July 12, 2007

